

Composites of Novel Biodegradable Copolyamides Based on Adipic Acid, 1,6-Hexane Diamine, and L-Glycine with Short E-Glass Fibers. II. Preparation and Properties

IOANNIS ARVANITTOYANNIS,^{1,*} ELENI PSOMIADOU,¹ NOBORU YAMAMOTO,¹ and JOHN M. V. BLANSHARD²

¹Osaka National Research Institute, AIST, Organic Materials Department, Functional Polymer Section, 1-8-31 Midorigaoka, Ikeda, 563 Osaka, Japan and ²University of Nottingham, Department of Food Science, Sutton Bonington Campus, Sutton Bonington, Leics LE12 5RD, Loughborough, England

SYNOPSIS

A study was conducted on the preparation of composite materials based on novel biodegradable copolyamides reinforced with E-glass fibers by using the hand lay-up technique. Differential thermal analysis (DTA) and wide angle x-ray diffraction patterns were employed for investigating the effect of transcrystallinity on percentage crystallinity of composites. The thermal properties of composites (T_g and T_m) were determined with DTA and dynamic mechanical thermal analyzer (DMTA) measurements. Void fractions were evaluated from density measurements and correlated to glass fiber contents. The stress-strain curves and compression strength measurements were recorded and correlated with the glass fiber content, void content, and the percentage amino acid content of the copolymers. Although high α -amino acid contents caused a decrease in T_g and T_m and the tensile strength of copolyamides, the introduction of glass fibers was found to counterbalance this effect by initiating an increase in the percentage crystallinity. © 1995 John Wiley & Sons, Inc.

INTRODUCTION

On several occasions, starch has been used with several synthetic nonbiodegradable polymers such as polyethylene and ethylene/acrylic acid copolymers PVA and PVC for preparing biodegradable paper-like composite materials.¹⁻⁶ In addition to starch a variety of other particulate materials such as cellulose, lignin, saw dust, casein, and mannitol also have been suggested as potentially degradable fillers.⁷ However it should be pointed out that in most of the above-mentioned cases probably only the natural poly/oligomer undergoes degradation thus leaving an almost unaltered porous and mechanically weakened, but practically undegraded synthetic polymer.⁸ Therefore, the development of novel biodegradable polymers and their use for preparation of composites, endowed with desirable structural

features and properties, have recently gained importance.⁹ Although D,L- or L-lactide and ϵ -caprolactone seem to be the most popular monomers especially in the field of polymeric composite materials,¹⁰⁻¹⁴ another promising class of polymers are the polyamides, whose applicability has been restricted because of the lack of biodegradability.^{15,16} Our previous publications reported on the statistical incorporation of α -amino acids in the polymeric chain of polyamides thus modifying, to some extent, the main polymeric backbone and making these polymers more susceptible to biodegradation.¹⁷⁻²⁰ This study investigates the effect of introducing short E-glass fibers in a series of copolyamides based on AA/1,6HD/L-glycine. Several previous publications in the same field reported on the preparation and properties of glass/carbon fiber thermoplastic homopolyamide composites.²¹⁻²⁵ The current study was mainly motivated by the continuous increase in demand of thermoplastic matrices as parts of novel environmentally degradable polymer composites. The inherent advantages of these materials over the majority of thermoset materials²⁶ such as the control

* To whom correspondence should be addressed. Current address: Dr. J. Arvanitoyannis, 92, Kassandrou, 54634 Thessaloniki, Greece.

of their percentage crystallinity (physicochemical properties),²⁷ ease of processing²¹ and environmental safety are expected to make them even more attractive from the application viewpoint.

EXPERIMENTAL

Materials

The copolyamides based on AA/1,6HD/L-glycine were those reported in previous publications.^{17,27} The short E-glass fibers were supplied by Ciba-Geigy S.A. The molar composition of the above-mentioned copolyamides and the characteristics of the short E-glass fibers are given in list 1 and list 2, respectively.

List 1 Molar Composition of Copolyamides Synthesized from Nylon 6,6 Salt and L-Glycine Currently Used as Matrices

AA (mol)	1,6HD (mol)	L-Glycine (mol)
50.0	50.0	0.0
47.5	47.5	5.0
45.0	45.0	10.0
42.5	42.5	15.0
40.0	40.0	20.0
37.5	37.5	25.0

List 2 Short E-Glass Fiber Characteristics (Ciba Geigy, S.A.)

Average fiber length	3 mm
Surface treatment	Nontreated
Density	2.54 g/cm ³
Tensile strength	3500 MPa
Elasticity modulus	38.98 GPa

Preparation of Copolyamide Composites: Hand Lay-Up Method

Both the molding box and the method for preparation of composites have been previously reported in detail.^{25,27} When the molding box was taken out of the furnace, it was cooled down by using three different approaches²⁸: quenched in ice water, cooled in the air at room temperature, and cooled gradually in the oven.

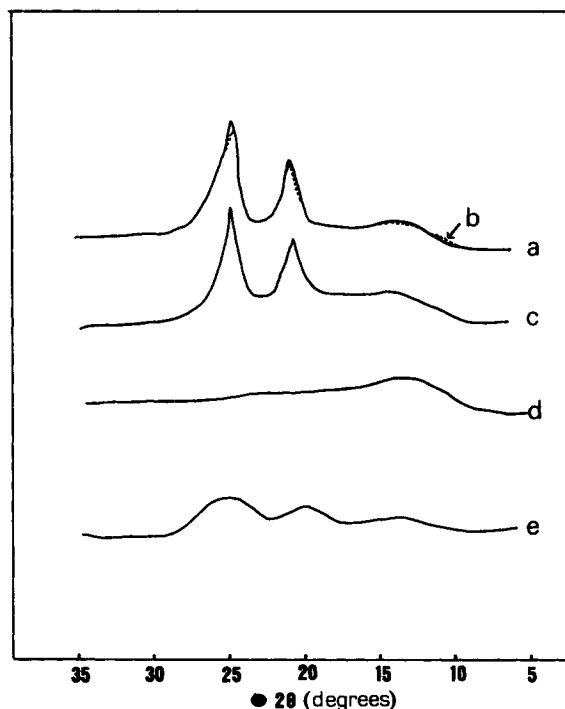


Figure 1 Comparison of experimental and calculated WAXDP for E-glass fiber-reinforced AA/1,6HD/L-glycine, 40/40/20 (expressed in % mol/mol/mol) copolyamides: (a) experimental; (b) calculated; (c) simulated 100% crystalline; (d) glass fiber; and (e) 100% amorphous.

Characterization of Neat Copolyamides and Copolyamide Composites

Density Measurements

Densities were determined at 23°C, pycnometrically^{29,30} using a density gradient column (Davenport, UK). The polymer samples were previously degassed at 0.1 mmHg for 2 h. The density column was constructed by using toluene and carbon tetrachloride with a density range of 0.99–1.40 g cm⁻³.

Differential Thermal Analysis (DTA) Measurements

The glass transitions (T_g) and the melting points (T_m) were determined using a DuPont differential thermal analyzer (DTA, 900) connected to an IBM computer PC/2 and a Hewlett-Packard Color Pro Plotter. The heating rate was 5°C/min and the temperature range was from -50°C to $T_m + 20$ °C. The calibration of temperature and heat enthalpy (J/g) of the DTA were made with indium. Five measurements were recorded per sample. T_g s were defined as the midpoints of step changes in heat capacities (ΔC_p); melting points and crystallization tempera-

Table I Percentage Crystallinity (% X_c) of Reinforced Copolyamides from WAXDP

AA/1,6HD/L-Glycine (mol/mol/mol)	% Glass Fiber Content	% X_c
50.0/50.0/0.0	0	32.8
	15	34.5
	30	39.2
	45	42.5
47.5/47.5/5.0	0	27.7
	15	29.4
	30	33.0
	45	36.6
45.0/45.0/10.0	0	23.0
	15	25.4
	30	28.1
	45	31.9
42.5/42.5/15.0	0	14.7
	15	18.0
	30	21.8
	45	25.0
40.0/40.0/20.0	0	5.6
	15	6.8
	30	8.3
	45	9.2
37.5/37.5/25.0	0	—
	15	—
	30	—
	45	—

tures were defined as the peaks of endothermic and exothermic curves, respectively.

Dynamic Mechanical Thermal Analysis (DMTA) Measurements

DMTA measurements were carried out using a PL-DMTA (MarkII, UK) connected to an Olivetti PC286 and a Hewlett-Packard Color Pro Plotter. The heating rate was 5°C/min; frequency, 1 Hz; and dimensions of the bars, 40 mm long, 7 mm wide, and 3.2 mm thick. $\tan \delta (=E''/E')$ and E'' (loss modulus) were defined as the peaks of the curves, whereas E' (storage modulus) was defined by the intersection of the extrapolations of the two linear parts.

Wide Angle X-Ray Diffraction Patterns (WAXDP)

WAXDP ($2\theta = 5\text{--}35^\circ$) were recorded using a Philips PW1050 diffractometer. Measurements were taken at 0.05° intervals with a counting time of 4 s. Five measurements were recorded per sample to ensure the reproducibility of our results.

Mechanical Properties

The tensile tests were conducted on a 5 ton Instron universal testing machine (TM-SM 1102, UK). The extension rate was maintained at 1 mm/min. The load elongation curves were plotted and tensile modulus, tensile strength, tensile stress, and percentage strain were calculated from the curves. Compression tests were also carried out and the force was recorded for the evaluation of the compressive strength. The tensile specimens were of the following geometry: 6 mm wide, 30 mm long, and 5 mm thick; the dimensions of the compressive specimens were 8 mm diameter and 32 mm height. A minimum of five measurements were recorded per sample.

Moisture Absorption

All specimens were first dried at 100°C over silica gel in a vacuum oven until constant weight. Then they were immersed in water in glass vessels thermostated at 20, 30, 40, 50, 60, 80, and 100°C. The latter (thermostated at 100°C) was equipped with a water condenser in order to avoid evaporation of water. Eventual weight gains were recorded after removing the specimens from the thermostated bath, and wiping the superficial moisture traces (by using a cloth), and finally weighing them periodically on a Chyo balance (Japan) with precision of 0.1 mg.

RESULTS AND DISCUSSION

WAXDP

The construction of the diffraction pattern of our composite material was made according to the following steps as reported elsewhere^{26,31,32}: record the diffraction pattern of the totally (100%) amorphous polymer (after having it quenched in liquid nitrogen); record the totally (100%) crystalline polymer; take the pattern of the reinforced phase; and after the required scaling up add the above three patterns together so that the composite pattern is formed. Therefore, the pattern of the semicrystalline composite material could be analyzed to its three components:

$$Q = Q_{\text{amor}} + Q_{\text{cryst}} + Q_{\text{fiber}} \quad (1)$$

where Q_{amor} is the integrated intensity of the amorphous phase; Q_{cryst} , the integrated intensity of the crystalline phase; and Q_{fiber} is the integrated intensity of the E-glass fiber.

Table II Thermal Properties for Copolyamides

AA/1,6HD/L-Glycine (mol/mol/mol)	% Glass Fiber Content	T_g (°C)	T_{m1} (°C)	T_{m2} (°C)	T_{m3} (°C)	ΔH_m (J/g)
50.0/50.0/0.0	0	58.2 ± 2.2	258.3 ± 3.8	245.0 ± 2.6	—	110.6 ± 1.3
	15	59.0 ± 3.1	260.0 ± 4.1	246.2 ± 2.0	227.2 ± 4.2	114.5 ± 2.5
	30	59.9 ± 1.5	261.5 ± 3.4	248.0 ± 3.5	228.6 ± 1.8	119.6 ± 3.6
	45	60.7 ± 2.0	262.7 ± 4.0	249.6 ± 2.5	231.2 ± 3.0	125.2 ± 4.2
47.5/47.5/5.0	0	53.0 ± 2.0	241.7 ± 2.0	230.1 ± 3.4	—	99.0 ± 3.8
	15	53.8 ± 1.3	243.3 ± 3.2	231.9 ± 4.2	213.2 ± 3.2	103.5 ± 2.7
	30	55.0 ± 2.2	244.6 ± 3.1	233.2 ± 3.1	214.5 ± 2.8	107.8 ± 3.5
	45	56.1 ± 1.9	245.4 ± 2.8	234.3 ± 2.6	216.3 ± 3.6	112.4 ± 4.1
45.0/45.0/10.0	0	52.6 ± 1.8	227.5 ± 2.1	215.4 ± 2.0	—	74.1 ± 2.3
	15	53.2 ± 2.5	228.8 ± 3.0	216.5 ± 3.2	200.4 ± 2.8	80.4 ± 4.5
	30	54.4 ± 3.0	230.0 ± 2.8	218.3 ± 2.6	201.5 ± 3.3	84.9 ± 3.9
	45	55.0 ± 2.1	230.9 ± 2.5	219.6 ± 2.5	202.6 ± 2.9	90.5 ± 2.6
42.5/42.5/15.0	0	50.1 ± 0.9	212.1 ± 1.8	200.4 ± 3.0	—	58.7 ± 1.8
	15	51.0 ± 1.8	213.4 ± 2.9	201.6 ± 3.6	183.7 ± 2.8	62.9 ± 2.6
	30	52.2 ± 2.4	214.7 ± 3.2	202.3 ± 2.1	184.9 ± 3.2	68.5 ± 3.2
	45	53.1 ± 3.2	215.9 ± 4.0	203.1 ± 2.5	186.2 ± 3.4	74.6 ± 2.6
40.0/40.0/20.0	0	49.8 ± 1.2	201.7 ± 1.9	—	—	47.0 ± 1.5
	15	50.6 ± 1.2	203.1 ± 2.8	195.2 ± 3.4	—	53.2 ± 3.0
	30	51.0 ± 3.1	204.5 ± 2.0	195.9 ± 2.5	—	58.5 ± 2.5
	45	51.6 ± 2.0	206.0 ± 3.5	196.8 ± 3.0	—	64.6 ± 3.3
37.5/37.5/25.0	0	48.4 ± 1.0	185.2 ± 2.2	—	—	45.8 ± 2.0
	15	49.0 ± 1.0	187.0 ± 3.5	178.3 ± 2.5	—	50.4 ± 3.5
	30	50.2 ± 3.3	188.1 ± 2.8	179.6 ± 3.1	—	56.2 ± 2.7
	45	50.7 ± 2.4	189.4 ± 3.0	180.5 ± 2.8	—	60.1 ± 3.8

Glass transitions, T_g ; melting points, T_m ; heats of fusion, ΔH_m . Results give the average and standard deviation of five measurements ($x \pm SD$).

Although we should bear in mind that in this model the 100% crystalline copolyamide pattern has to be simulated and preparation of the randomly oriented glass fiber reinforced copolyamides is assumed,³¹⁻³⁴ the advantage of this model consisting of reliable and reproducible determination of percentage crystallinity should be equally stressed. Figure 1 shows curves of neat copolyamide AA/1,6HD/L-glycine (40/40/20) expressed in (% mol/mol/mol), traces of amorphous copolymers (quenched in water), E-glass fiber, and their composites (glass fiber with the above-mentioned copolymers). Both the neat copolyamide patterns and their E-glass fiber composites were fit as previously^{26,32} by simulating the main peaks within the range of 5–35°. Figure 1 shows schematically a representative application of the method for “constructing” the “calculated” copolyamide composite. The results of percentage crystallinity for the glass fiber reinforced AA/1,6HD/L-glycine copolyamides are given in Table I. A gradual increase in the percentage crystallinity (recorded from WAXDP) with higher glass fiber content was observed.

DTA

It is well established that the character of the interface is of great significance to the adhesion between fiber and matrix in a composite material.³⁵ The occurrence of nucleation fronts on the glass fiber, in addition to the statistical nucleation from the melt, is indicated as “transcrystallinity.” Although there has been a long controversy³⁵⁻³⁷ over the positive or negative effect of transcrystallinity on adhesion and mechanical properties, DTA measurements show the appearance of several (two or three) melting peaks that could be attributed, as previously suggested,^{26,38} to various spherulite morphologies resulting from constrained growth in thermoplastic composites, that is, high and low nucleating density, respectively. The occurrence of two antagonizing tendencies toward the crystallization that is enhancement of crystallization by providing nuclei, and at the same time constraining the growth by an impingement mechanism, complicates our understanding of the system. An attempt was recently made to separate these two effects with computer simulation.³⁹

Table III Effect of Cooling Conditions on Density (ρ), Void Fraction (ν), and Percentage Crystallinity ($\%X_c$) of Copolyamide Reinforced with Glass Fibers

AA/1,6HD/L-Glycine (mol/mol/mol)	% Glass Fiber Content	Measured Density (g/cm ³)	Calculated ^a Density (g/cm ³)	Void ^b Fraction (ν)	$\%X_c^c$
Ice water					
50.0/50.0/0.0	0	1.1184	—	—	18.5
	15	1.1730	1.2206	0.039	23.6
	30	1.2601	1.3434	0.062	28.8
	45	1.3069	1.4936	0.125	32.7
47.5/47.5/5.0	0	1.1297	—	—	15.0
	15	1.1901	1.2320	0.034	17.4
	30	1.2830	1.3548	0.053	21.5
	45	1.4872	1.5047	0.116	24.3
45.0/45.0/10.0	0	1.1364	—	—	9.8
	15	1.1992	1.2388	0.032	13.4
	30	1.3002	1.3615	0.045	18.0
	45	1.3586	1.5112	0.101	22.1
42.5/42.5/15.0	0	1.1472	—	—	3.8
	15	1.2235	1.2497	0.021	6.8
	30	1.3285	1.3724	0.032	12.5
	45	1.3984	1.5217	0.081	16.2
37.5/37.5/25.0	0	1.1651	—	—	—
	15	1.2487	1.2677	0.015	—
	30	1.3583	1.3903	0.023	—
	45	1.4404	1.5389	0.064	—
Oven cooled					
50.0/50.0/0.0	0	1.1383	—	—	43.4
	15	1.2171	1.2407	0.019	45.8
	30	1.3075	1.3634	0.041	49.5
	45	1.3709	1.5131	0.094	56.0
47.5/47.5/5.0	0	1.1446	—	—	38.5
	15	1.2309	1.2471	0.013	41.9
	30	1.3509	1.3984	0.034	46.3
	45	1.3977	1.5192	0.080	50.4
45.0/45.0/10.0	0	1.1585	—	—	30.4
	15	1.2498	1.2611	0.009	35.3
	30	1.3491	1.3837	0.025	41.0
	45	1.4345	1.5326	0.064	45.8

The glass transitions (T_g), melting points ($T_{m,1}$, $T_{m,2}$, $T_{m,3}$), and heats of fusion (ΔH_m) of the composites for E-glass fiber reinforced AA/1,6HD/L-glycine copolyamides are given in Table II. It should be mentioned that primary (initial) and secondary nucleation were considered responsible for the occurrence of multiple peaks observed in several homo- and copolyamide composites.^{26,32,40} Previous studies on thermal properties (DTA) of nylon 6,6 and biodegradable copolyamides reinforced with E-glass fibers also confirmed the bimodal endotherm peak attributed to thermodynamically and kinetically favored crystal formation in agreement with these experiments.^{32,40} The effect of transcrystallinity on the heats of fusion

(Table II) can be understood if the latter are correlated with the fiber nucleation density. The presence of many more nucleation sites (transcrystallinity effect)³⁹ due to high fiber nucleation density resulted in a decrease of the average spherulite size.

The effect of several cooling modes on percentage crystallinity was investigated and the results are given in Table III. It is evident that slow cooling rates promote higher crystallinities by leading to the formation of more perfect crystals, but the fast cooling rates (i.e. quenching) have an adverse effect upon the development of crystallinity. Similar results were obtained for the copolyamides (nylon 6/nylon 12) and copolyam-

Table III *Continued*

AA/1,6HD/L-Glycine (mol/mol/mol)	% Glass Fiber Content	Measured Density (g/cm ³)	Calculated ^a Density (g/cm ³)	Void ^b Fraction (ν)	% X _c ^c
42.5/42.5/15.0	0	1.1653	—	—	21.2
	15	1.2591	1.2680	0.007	26.6
	30	1.3598	1.3904	0.022	31.4
	45	1.4514	1.5391	0.057	36.2
37.5/37.5/25.0	0	1.1890	—	—	—
	15	1.2853	1.2918	0.005	—
	30	1.3885	1.4140	0.018	—
	45	1.4852	1.5617	0.049	—
Air cooled					
50.0/50.0/0.0	0	1.1270	—	—	33.4
	15	1.1924	1.2293	0.030	36.0
	30	1.2831	1.3521	0.051	39.8
	45	1.3384	1.5021	0.109	44.3
47.5/47.5/5.0	0	1.1365	—	—	28.9
	15	1.2092	1.2389	0.024	32.5
	30	1.3031	1.3616	0.043	36.8
	45	1.3647	1.5113	0.097	40.7
45.0/45.0/10.0	0	1.1452	—	—	22.6
	15	1.2227	1.2477	0.020	26.4
	30	1.3183	1.3704	0.038	31.8
	45	1.38	1.5197	0.088	38.0
42.5/42.5/15.0	0	1.1572	—	—	13.8
	15	1.2422	1.2598	0.014	17.5
	30	1.3465	1.3824	0.026	21.8
	45	1.4241	1.5313	0.070	25.5
37.5/37.5/25.0	0	1.1765	—	—	—
	15	1.1769	1.2792	0.008	—
	30	1.3736	1.4016	0.020	—
	45	1.4631	1.5499	0.056	—

Results give the average of five measurements.

^a Calculated according to eq. (3).

^b Calculated according to eq. (2).

^c Determined from WAXDP.

ides AA/1,6HD/L-proline reinforced with E-glass fibers.^{26,32}

Density Measurements: Detection of Void Content

The main purpose for carrying out the density measurements was to determine the void volume fraction. The most important factors, generally considered responsible for promoting the occurrence of voids in polymer composites are the following: possible entrapment of air within compounded pelletized material, residual moisture, and shrinkage of volume of the core region.^{26,41,42} The void volume fraction (ν) was calculated from the measured (p) and calculated (p_{calc}) composite densities as follows:

$$\nu = 1 - \frac{p}{p_{\text{calc}}} \quad (2)$$

The solid, void-free density of the composite (p_{compos}) was calculated from the density of the pure copolyamide (p_p) and that of the glass fiber (p_f) as shown in eq. (3):

$$p_{\text{compos}} = \frac{p_f p_p}{(1 - w_f)p_f + w_f p_p} \quad (3)$$

where w_f is the glass fiber weight fraction (determined by burning off the copolyamide). The results of the density values for neat and glass fiber reinforced composites and the void fraction and percentage crystallinity (from WAXDP) developed

Table IV Theoretical and Experimental Ultimate Tensile Strength Values for Copolyamide Composites

AA/1,6HD/L-Glycine (mol/mol/mol)	% Glass Fiber Content	Tensile Strength (MPa)																		
		Experimental	Calculated According to				Corrected Multi- Coeff. Instead of 0.7	Calculated According to				Corrected Multi- Coeff. Instead of 0.7								
			Eq. (4)	Eq. (5)	Eq. (5)	Eq. (5)		Eq. (6)	Eq. (6)	Eq. (6)	Eq. (6)									
50.0/50.0/0.0	0	83 ± 4	—	—	—	—	—	—	—	—	—	—	—	—	—	—	—	—	—	—
	15	215 ± 7	254	367	187	349	185	0.51	349	185	0.37	349	185	0.37	349	185	0.37	349	185	0.37
	30	373 ± 12	425	735	375	723	382	0.51	723	382	0.37	723	382	0.37	723	382	0.37	723	382	0.37
	45	493 ± 11	596	1102	562	1116	590	0.51	1116	590	0.37	1116	590	0.37	1116	590	0.37	1116	590	0.37
	0	78 ± 5	—	—	—	—	—	—	—	—	—	—	—	—	—	—	—	—	—	—
47.5/47.5/5.0	15	189 ± 10	250	367	176	349	165	0.47	349	165	0.33	349	165	0.33	349	165	0.33	349	165	0.33
	30	344 ± 21	422	735	346	723	341	0.47	723	341	0.33	723	341	0.33	723	341	0.33	723	341	0.33
	45	462 ± 15	594	1102	518	1116	526	0.47	1116	526	0.33	1116	526	0.33	1116	526	0.33	1116	526	0.33
	0	70 ± 4	—	—	—	—	—	—	—	—	—	—	—	—	—	—	—	—	—	—
	15	172 ± 8	243	367	158	349	155	0.43	349	155	0.31	349	155	0.31	349	155	0.31	349	155	0.31
45.5/45.0/10.0	30	315 ± 16	416	735	316	723	320	0.43	723	320	0.31	723	320	0.31	723	320	0.31	723	320	0.31
	45	434 ± 23	589	1102	474	1116	494	0.43	1116	494	0.31	1116	494	0.31	1116	494	0.31	1116	494	0.31
	0	61 ± 6	—	—	—	—	—	—	—	—	—	—	—	—	—	—	—	—	—	—
	15	153 ± 6	235	367	147	349	140	0.40	349	140	0.28	349	140	0.28	349	140	0.28	349	140	0.28
	30	287 ± 12	410	735	294	723	289	0.40	723	289	0.28	723	289	0.28	723	289	0.28	723	289	0.28
42.5/42.5/15.0	45	405 ± 20	584	1102	441	1116	446	0.40	1116	446	0.28	1116	446	0.28	1116	446	0.28	1116	446	0.28
	0	50 ± 4	—	—	—	—	—	—	—	—	—	—	—	—	—	—	—	—	—	—
	15	138 ± 9	226	367	125	349	125	0.34	349	125	0.25	349	125	0.25	349	125	0.25	349	125	0.25
	30	253 ± 13	402	735	250	723	258	0.34	723	258	0.25	723	258	0.25	723	258	0.25	723	258	0.25
	45	378 ± 16	578	1102	375	1116	399	0.34	1116	399	0.25	1116	399	0.25	1116	399	0.25	1116	399	0.25
40.0/40.0/20.0	0	38 ± 3	—	—	—	—	—	—	—	—	—	—	—	—	—	—	—	—	—	—
	15	107 ± 5	216	367	110	349	105	0.30	349	105	0.21	349	105	0.21	349	105	0.21	349	105	0.21
	30	220 ± 15	394	735	220	723	217	0.30	723	217	0.21	723	217	0.21	723	217	0.21	723	217	0.21
	45	334 ± 11	572	1102	331	1116	335	0.30	1116	335	0.21	1116	335	0.21	1116	335	0.21	1116	335	0.21
	0	—	—	—	—	—	—	—	—	—	—	—	—	—	—	—	—	—	—	—

Experimental results give the average and the standard deviation of five measurements (x ± SD).

Table V Theoretical and Experimental Tensile Moduli Values and Compressive Strength of Copolyamides Reinforced with Glass Fibers

AA/1,6HD/L-Glycine (mol/mol/mol)	% Glass Fiber Content	Tensile Modulus (GPa)			Compressive Strength (MPa)					Correction Coeff. Instead of 0.63	
		Theoret. Lower Limit According to Eq. (8)	Theoret. Upper Limit According to Eq. (7)	Experimental	Theoretically Calculated According to						
					Eq. (9)	Eqs. (10), (11)	Modified Eqs. (10), (11)				
50.0/50.0/0.0	0	—	—	2.10 ± 0.15	—	—	87.3 ± 4.2	—	—	—	—
	15	2.45	7.63	3.28 ± 0.20	—	658	120.1 ± 5.8	533	93	—	0.174
	30	2.93	13.16	6.79 ± 0.19	—	2052	172.5 ± 7.3	647	179	—	0.174
	45	3.66	18.70	8.45 ± 0.32	—	4255	280.9 ± 6.5	823	227	—	0.174
	0	—	—	2.15 ± 0.13	—	—	75.1 ± 2.9	—	—	—	—
47.5/47.5/5.0	15	2.51	7.68	3.10 ± 0.15	—	666	105.4 ± 3.8	546	134	—	0.155
	30	3.00	13.20	6.31 ± 0.22	—	2077	157.8 ± 5.2	663	163	—	0.155
	45	3.74	18.73	7.98 ± 0.17	—	4305	258.9 ± 6.5	843	207	—	0.155
	0	—	—	2.06 ± 0.18	—	—	62.4 ± 3.4	—	—	—	—
	15	2.40	7.60	2.85 ± 0.21	—	652	94.8 ± 4.5	523	119	—	0.143
45.5/45.0/10.0	30	2.88	13.14	5.98 ± 0.20	—	2033	135.0 ± 2.8	635	144	—	0.143
	45	3.59	18.68	7.60 ± 0.24	—	4214	232.4 ± 3.3	808	184	—	0.143
	0	—	—	1.91 ± 0.20	—	—	50.0 ± 4.6	—	—	—	—
	15	2.23	7.47	2.60 ± 0.31	—	628	83.4 ± 5.9	462	104	—	0.142
	30	2.67	13.03	5.73 ± 0.10	—	1957	120.8 ± 2.8	562	127	—	0.142
42.5/42.5/15.0	45	3.34	18.59	7.39 ± 0.12	—	4058	199.9 ± 4.0	715	161	—	0.142
	0	—	—	1.75 ± 0.12	—	—	37.5 ± 2.3	—	—	—	—
	15	2.04	7.33	2.49 ± 0.16	—	601	72.8 ± 4.8	444	94	—	0.133
	30	2.45	12.92	5.38 ± 0.20	—	1873	110.0 ± 5.5	539	114	—	0.133
	45	3.07	18.51	7.06 ± 0.17	—	3884	180.4 ± 4.0	686	145	—	0.133
40.0/40.0/20.0	0	—	—	1.53 ± 0.09	—	—	26.3 ± 4.0	—	—	—	—
	15	1.79	6.69	2.36 ± 0.19	—	562	65.5 ± 4.5	388	83	—	0.135
	30	2.15	12.77	5.03 ± 0.24	—	1752	98.0 ± 5.2	472	101	—	0.135
	45	2.70	18.38	6.72 ± 0.27	—	3632	159.8 ± 6.0	600	129	—	0.135
	0	—	—	—	—	—	—	—	—	—	—

Experimental results give the average and the standard deviation of five measurements ($\bar{x} \pm SD$).

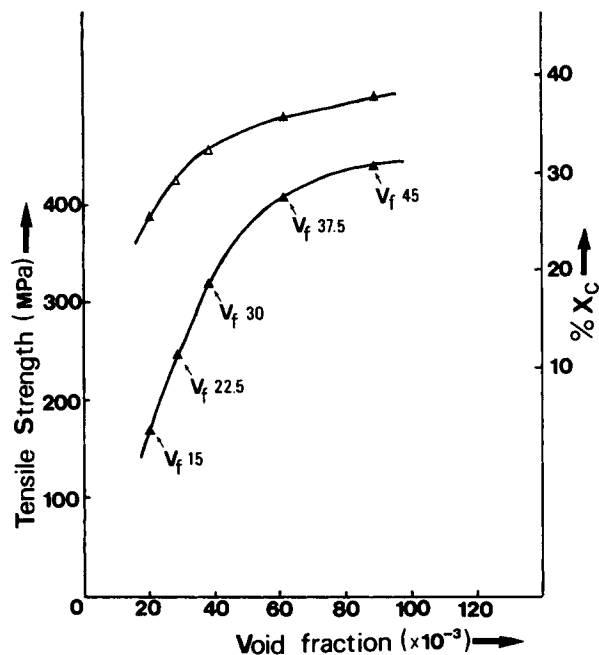


Figure 2 Tensile strength and percentage crystallinity (% X_c) against the void fraction of AA/1,6HD/L-glycine (45/45/10 expressed in % mol) composites of various fiber contents, $V_f = 15$ –45%.

at three different cooling rates are given in Table III.

The observed increase in void volume fraction with glass fiber content (Table III) has been reported in previous publications^{26,28,42} and attributed to various factors such as insufficient adhesion of the polymer matrix to the E-glass fibers, deformation of crystals, transcrystallinity,^{32,42} and bubble formation.^{43,44} The results obtained from our study on the effect of different cooling modes on the density and void content are in agreement with previous studies³² that showed that the higher void contents are related to very fast cooling. Therefore the higher void content order is as follows: quenching in ice water > air cooled > oven cooled. The drastic cooling conditions imposed upon the composite material when quenched in ice water could result in external partial surface solidification but the interior cannot be freely contracted thus resulting in undesirable high internal void contents as previously reported.^{26,32}

Mechanical Properties

Tensile Strength

An increase in the glass fiber content was always related to an increase in the tensile strength of the

copolyamide composites. It is noteworthy that the stress-strain curves of the composites were essentially linear and showed only a slight curvature near the breaking point; the neat copolyamides showed definite yield points before their fracture. Table IV summarizes the results derived from the stress-strain curves and the compressive strength-time (distance) plots both for neat and E-glass fiber reinforced copolyamides.

Theoretical calculations of the tensile strength for the glass fiber reinforced copolyamides were carried out according to the following equations (presuppositions for the applicability of which were given previously²⁶). (i) Rule of mixtures:

$$\sigma_u = n\sigma_f V_f + \sigma_m(1 - V_f) \quad (4)$$

where σ_u is the tensile strength of the composite; σ_f , the tensile strength of the glass fiber; σ_m , the tensile strength of the matrix (in our case copolyamide); V_f , the fiber volume fraction; and n , the Krenchel's efficiency factor ($n = 0.5$ for crossply fiber composites).^{25,26} (ii) Weibull's simplified equation:

$$\sigma_u = 0.7\sigma_f V_f \quad (5)$$

and (iii) Dow and Rosen's analysis (cited by Shrivastava and Lal²⁵) that resulted in the following formula:

$$\sigma_u = \sigma_r V_f \left[\frac{(1 - V_f)^{0.5}}{V_f^{0.5}} \right]^{-1/2\beta} \quad (6)$$

where σ_r is the reference stress level depending on the particular combination of fiber and matrix (copolyamide in our case) properties and β is a statistical parameter of the Weibull distribution related to the fiber strength, which is equal to 7.7 for commercial E-glass fiber.²⁵

Comparing the experimental results to those obtained from eqs. (4)–(6) it was found that only the modified eq. (5) gives a good fit to the experimental results, as previously reported,^{25,26,32} but eqs. (4) and (6) fail to provide a good fit. Reasons possibly advocated for these discrepancies include the high hygroscopicity of the copolyamide matrix (because of α -amino acid as comonomer unit), the void content, and eventual fiber misalignment due to usage of multifiber strands.^{45–47} The fracture of the composites is believed to have been originally initiated by matrix failure near fiber ends followed by a transversal crack propagation that results in fracture of composite without necessitating the breaking of the

Table VI Effect of Moisture Conditioning on Thermal Properties of Copolyamides Composites

AA/1,6HD/L-Glycine (mol/mol/mol)	% Glass Fiber Content	T_g (°C)	T_m (°C)	ΔH_m (J/g)	E_a (kJ/mol)
50.0/50.0/0.0	0	56.0 ± 2.3	256.1 ± 2.5	106.5 ± 2.4	52.0
	15	57.8 ± 2.7	258.0 ± 3.2	111.3 ± 1.9	60.5
	30	58.7 ± 3.1	259.4 ± 2.8	117.7 ± 2.2	68.8
	45	59.9 ± 2.0	260.8 ± 2.0	123.9 ± 2.0	78.2
47.5/47.5/5.0	0	50.2 ± 1.8	238.1 ± 1.8	94.2 ± 2.3	48.8
	15	52.7 ± 2.3	240.3 ± 1.5	100.9 ± 2.3	56.7
	30	53.9 ± 1.5	242.9 ± 2.4	105.3 ± 1.8	63.2
	45	55.2 ± 1.8	243.8 ± 2.2	110.8 ± 2.4	71.5
45.0/45.0/10.0	0	49.1 ± 2.1	223.7 ± 2.4	67.2 ± 1.8	46.3
	15	51.6 ± 3.0	225.2 ± 1.8	76.1 ± 2.0	52.5
	30	53.0 ± 2.5	227.7 ± 2.3	81.3 ± 1.7	58.4
	45	53.5 ± 2.3	228.6 ± 1.5	87.9 ± 1.9	65.4
42.5/42.5/15.0	0	46.9 ± 2.5	207.0 ± 2.4	51.0 ± 2.3	44.8
	15	48.7 ± 2.0	208.7 ± 2.6	57.8 ± 1.8	50.3
	30	50.2 ± 2.3	209.8 ± 3.1	64.7 ± 2.0	54.8
	45	51.3 ± 2.7	212.9 ± 2.0	71.2 ± 2.5	63.9
40.0/40.0/20.0	0	45.4 ± 1.9	195.1 ± 2.4	38.8 ± 1.8	43.6
	15	47.8 ± 2.5	197.0 ± 3.2	47.1 ± 2.3	47.5
	30	49.0 ± 2.7	198.5 ± 1.2	53.8 ± 2.6	53.4
	45	49.8 ± 2.2	202.1 ± 1.0	60.9 ± 1.9	62.4
37.5/37.5/25.0	0	44.3 ± 2.6	176.2 ± 2.2	37.0 ± 1.3	39.8
	15	46.0 ± 2.5	180.3 ± 1.5	43.7 ± 2.0	43.5
	30	47.1 ± 2.1	181.7 ± 1.8	50.2 ± 1.2	50.1
	45	48.3 ± 2.4	183.9 ± 1.1	55.9 ± 1.1	57.4

Determination of water diffusion activation energies (E_a); results give the average and standard deviation of five measurements ($x \pm SD$).

glass fibers as was observed on several occasions. The above suggestion is corroborated by the results of computer simulation on fracture mechanics of composite materials⁴⁸ and by SEM analysis on polyamides reinforced with short glass E-fibers reported previously.⁴⁹

Tensile Modulus

It was previously shown²⁶ that two estimates are available for tensile modulus (E_{compos}) of the glass fiber reinforced copolyamides. Depending solely on the direction of the applied stress with regard to the fiber orientation in the copolyamide composite, eqs. (7) and (8) were applied for upper and lower limits, respectively.

$$E_{\text{compos}} = V_f E_f + (1 - V_f) E_m \quad (7)$$

$$E_{\text{compos}} = \frac{1}{\left[\frac{V_f}{E_f} + \left(\frac{1 - V_f}{E_m} \right) \right]} \quad (8)$$

The results of the estimates and the experimentally found values for tensile moduli are given in Table V. The first observation is that the higher the contribution of the α -amino acid in the copolyamide, the weaker the matrix becomes, thus resulting in a much easier failure of the copolyamide reinforced with short glass fibers. The experimental values are shifted closer to the lower estimate [eq. (8)] probably because of the inherent complexity of short fiber reinforced thermoplastics because they consist of misaligned arrays of variable length fibers, dispersed in a viscoelastic matrix.^{50,51} The lowest extent of discrepancies between theoretical and experimental values was observed for the copolyamides containing the lowest glass fiber amount.

Figure 2 shows a correlation of the tensile strength with the void content and the percentage crystallinity developed at various cooling modes (see Tables III, IV). It is clear that high fiber contents result in high void contents that are also related to high percentage crystallinities and high tensile strength.

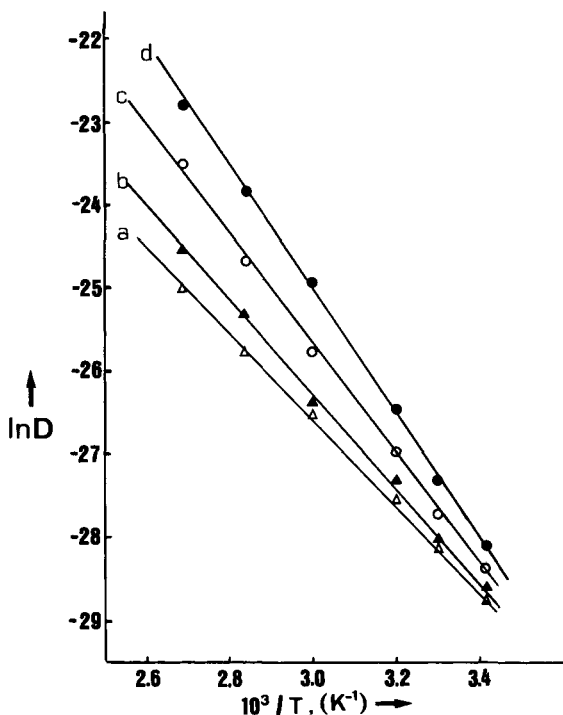


Figure 3 Arrhenius plots to determine the apparent activation energies for water diffusion for the (a) neat copolyamide AA/1,6HD/L-glycine (40/40/20 expressed in % mol/mol/mol) and its glass fiber composites (b) $V_f = 15\%$, (c) $V_f = 30\%$, and (d) $V_f = 45\%$.

Compression Strength

The compression strength was calculated by using the following three equations:

$$\sigma_{ce} = 2V_f \left[\frac{V_f E_m E_f}{3(1 - V_f)} \right]^{0.5} \quad (9)$$

$$\sigma_{cs} = \frac{G_m}{1 - V_f} \quad (10)$$

$$G_m = \frac{E_m}{2(1 + \nu)} \quad (11)$$

where σ_{ce} is the compression strength in the extension mode; σ_{cs} , the compression strength in the shear mode; E_m , the modulus of the elasticity of the matrix (copolyamides); E_f , the modulus of the elasticity of the fiber (glass fiber); G_m , the shear modulus; and ν is the Poisson ratio (dimensionless) equivalent to 0.44 for nylon 6,6.⁵²

Only after the introduction of a correction factor in eq. (10) can this equation provide a good fit for the experimental values. Depending on the kind of the matrix/fiber system, the correction coefficient was found to vary substantially, i.e. from 0.100 for

copolyamide/glass fiber²⁶ up to 0.63 for epoxy/boron composites.⁵³ In this case the correction coefficient was in the range (0.133–0.174) that is in satisfactory agreement with our previous investigation on nylon 6,6/glass fiber composites²⁶ and degradable composites.³² Both experimentally and theoretically calculated values for tensile and compression strength are given in Table V.

Hygrothermal Aging

Diffusion, capillarity, and transport by microcracks are the main mechanisms via which moisture penetration can occur within composite materials.⁵⁴ The rate of moisture absorption by a polymeric composite is mainly affected by the following factors: type of matrix and fiber, the fiber orientation with respect to the direction of diffusion, the conditioning temperature, the difference in water concentration between the composite and the environment and whether or not the absorbed water reacts chemically with the matrix.⁵⁰ The diffusivity or diffusion coefficient D , can be calculated from the following simplified equation that corresponds to the initial linear portion of the absorption curve:

$$\frac{M_t}{M_m} = \frac{4}{\pi^{1/2}} \left(\frac{Dt}{h^2} \right)^{1/2} \quad (12)$$

where M_t and M_m are mass of water absorbed at time t and at saturation, respectively and h is the thickness of infinitely large plates.

However if the diffusion is Fickian or only a function of temperature, it can be described with an Arrhenius relationship:

$$D = D_0 \exp(-E_a/RT) \quad (13)$$

where D_0 is the preexponential coefficient, or permeability index, R , E_a , and T are the gas constant, activation energy, and absolute temperature, respectively.

The moisture absorption was determined by the following equation:

$$M_t(\%) = \frac{(W - W_d)}{W_d} \times 100 \quad (14)$$

where W_d and W denote the weight of dry material (i.e. the initial weight of the material prior to exposure to the environment) and weight of moist material, respectively. The percentage equilibrium moisture absorption, M_m , was calculated as an av-

Table VII Effect of Moisture Conditioning (80°C, 7 Days) on Tensile Strength, Tensile Modulus, and Compression Strength of Copolyamides Reinforced with Glass Fibers

AA/1,6HD/L-Glycine (mol/mol/mol)	% Glass Fiber Content	Tensile Strength (MPa)	Tensile Modulus (GPa)	Compression Strength (MPa)
50.0/50.0/0.0	0	68 ± 4	1.13 ± 0.21	72.5 ± 2.92
	15	185 ± 16	2.51 ± 0.17	97.2 ± 6.80
	30	350 ± 18	6.20 ± 0.15	149.4 ± 5.21
	45	475 ± 23	8.15 ± 0.22	233.6 ± 6.70
47.5/47.5/5.0	0	48 ± 6	1.00 ± 0.1	59.2 ± 4.13
	15	121 ± 10	2.14 ± 0.20	74.6 ± 5.09
	30	285 ± 12	5.72 ± 0.35	120.0 ± 6.70
	45	422 ± 14	7.15 ± 0.33	196.2 ± 8.52
45.0/45.0/10.0	0	35 ± 4	0.88 ± 0.09	47.4 ± 1.34
	15	103 ± 7	1.70 ± 0.13	65.3 ± 3.00
	30	224 ± 11	5.15 ± 0.28	103.7 ± 4.82
	45	296 ± 17	6.53 ± 0.38	159.8 ± 4.70
42.5/42.5/15.0	0	23 ± 2	0.75 ± 0.05	32.0 ± 2.22
	15	82 ± 6	1.20 ± 0.08	53.5 ± 3.34
	30	154 ± 9	4.51 ± 0.30	91.3 ± 4.50
	45	220 ± 18	6.00 ± 0.37	137.8 ± 6.28
40.0/40.0/20.0	0	20 ± 3	0.62 ± 0.03	21.5 ± 1.37
	15	69 ± 8	1.05 ± 0.08	38.9 ± 2.80
	30	110 ± 7	4.06 ± 0.15	73.8 ± 5.35
	45	191 ± 16	5.33 ± 0.27	107.0 ± 8.42
37.5/37.5/25.0	0	14 ± 2	0.39 ± 0.02	13.1 ± 0.45
	15	43 ± 3	0.83 ± 0.09	32.0 ± 1.76
	30	92 ± 6	3.69 ± 0.13	45.7 ± 3.21
	45	140 ± 8	5.01 ± 0.32	87.9 ± 6.45

Results give the average and standard deviation of five measurements ($\bar{x} \pm SD$).

average value of several consecutive measurements that showed no appreciable additional absorption.

It should be mentioned that the DTA curves of AA/1,6HD/L-glycine copolyamides and their glass fiber reinforced composites before and after moisture absorption did not show any significant change within the first 24 h but, gradually, they began to show lower T_m and ΔH_m values. It is thought that when the samples are being subjected to moisture absorption the latter initiates a small scale reorganization of the molecules eventually resulting in local disruptions of the ordered structure (similarly to nylon 6,6⁵⁰) that can be easily observed in terms of differences in heats of fusion. The melting points and heats of fusion of the neat AA/1,6HD/L-glycine copolyamides and their glass fiber reinforced composites after their moisture conditioning, are given in Table VI.

The plots of $\ln D$ versus the inverse of absolute temperature ($1/T$) for the neat and reinforced copolyamides with L-glycine contents are shown in Figure 3. High L-glycine contents promote lower activation energies because of the hydrophilicity im-

parted upon the polymeric chain by the incorporation of L-glycine units. The diffusion activation energies (E_a) both for neat and glass fiber reinforced copolyamides are given in Table VI. A satisfactory agreement was found between the determined E_a (kJ/mol) values and previously reported values (55–61 kJ/mol)^{32,50,55} although they seem to be somewhat lower for copolyamides rich in L-glycine (40–57 kJ/mol) and rather higher (57–78 kJ/mol) for the copolyamides with high glass fiber content. Although the presence of fibers could, in theory, promote two minor mechanisms of moisture absorption, namely via capillarity or transport by microcracks, the experimentally determined high activation energies for moisture absorption show that the effect of transcrystallinity in conjunction with the lack of moisture absorption by the fibers⁴⁷ have the edge over the above-mentioned moisture absorption mechanisms.

Table VII gives us an insight in the effect of moisture conditioning (at 80°C for 7 days) on the mechanical properties (stress–strain curves) for both unreinforced and reinforced AA/1,6HD/L-glycine copolyamides. It is interesting that despite the low

(for achieving drastic changes in percentage crystallinity)⁵⁶⁻⁵⁸ conditioning temperature of our reinforced copolyamides, measurements of tensile strength, tensile modulus, and compression strength gave lower values for conditioned samples than for the dry ones thus indicating the synergistic action of plasticization of the matrix⁵⁷ (hydrophilic copolyamide in this case) and probably some limited degradation of the polymer-fiber interface (debonding) as well. Similar results were reported for the short glass fiber reinforced environmentally degradable composites³² and nylon 6,6 composites further supported with fractographic studies.⁴⁷ However, additional experimentation with scanning electron microscopy is required for examining the strength of the glass fiber copolyamide interfacial bond and for an in depth study of the prevailing fracture mechanism.

CONCLUSIONS

A series of composites based on novel biodegradable copolyamides reinforced with short E-glass fibers were prepared and their thermal and mechanical properties were evaluated both before and after moisture conditioning. Although various theoretical models concerning the prediction of mechanical properties and the moisture absorption were applied, modifications were necessitated for attaining better fit with the experimental results. The transcrystallinity effect was observed in thermal properties as appearance of multiple peaks, in mechanical properties (higher tensile and compression strength) and limited diffusion of water due to crystal formation.

REFERENCES

1. R. F. Storey and K. A. Shoemaker, *Polym. Bull.*, **31**, 331 (1993).
2. D. Satyanarayana and P. R. Chatterji, *J.M.S.—Rev. Macromol. Chem. Phys.*, **C33**, 349 (1993).
3. F. H. Otey, R. P. Westhoff, and C. R. Russell, *Ind. Eng. Chem., Proc. Res. Dev.*, **16**, 305 (1977).
4. G. J. L. Griffin and H. Mivetchi, *Proceedings of the 3rd International Biodegradation Symposium*, J. M. Sharpley and A. M. Kaplan, Eds., Applied Science, Essex, England, 1976.
5. G. J. L. Griffin, in *Fillers and Reinforcements for Plastics*, R. D. Deanin and N. R. Scott, Eds., ACS, Washington, DC, 1974, p. 159.
6. G. J. L. Griffin, *Am. Chem. Soc., Div. Org. Coatings, Plast. Chem. Pap.*, **33**, 78 (1973).
7. A. C. DeVisser, J. P. W. Vermeiden, and K. De Groot, in *Mechanical Properties of Biomaterials*, G. W. Hastings and D. F. Williams, Eds., Wiley, New York, 1980, p. 507.
8. W. Schnabel, *Polymer Degradation: Principles and Practical Applications*, Hanser International, Munchen, 1981 pp. 154-157.
9. G. S. Kumar, *Biodegradable Polymers: Prospects and Progress*, Marcel Dekker Inc., New York and Basel, 1987, pp. 1-40.
10. Ph. Dubois, I. Bakarar, R. Jerome, and Ph., Teyssie, *Macromolecules*, **26**, 4407 (1993).
11. S. M. Li, H. Garreau, and M. Vert, *J. Mater. Sci.: Mater. Med.*, **1**, 123 (1990).
12. S. M. Li, H. Garreau, and M. Vert, *J. Mater. Sci.: Mater. Med.*, **1**, 131 (1990).
13. S. M. Li, H. Garreau, and M. Vert, *J. Mater. Sci.: Mater. Med.*, **1**, 198 (1990).
14. C. C. P. Verheyen, C. P. A. T. Klein, J. M. A. de Blickehogervorst, J. G. C. Wolke, and C. A. van Blit-terwijn, *J. Mater. Sci.: Mater. Med.*, **4**, 58 (1993).
15. K. E. Gonsalves, X. Chen, and J. A. Cameron, *Macromolecules*, **25**, 3309 (1992).
16. Y. Tokiwa and T. Suzuki, *J. Appl. Polym. Sci.*, **26**, 441 (1981).
17. I. Arvanitoyannis, E. Nikolaou, and N. Yamamoto, *Proceedings of International Scientific Workshop on Biodegradable Plastics and Polymers*, Osaka, Nov. 1993, Y. Doi and K. Fukuda, Eds., Elsevier, Amsterdam, 1994, pp. 562-569.
18. I. Arvanitoyannis, E. Nikolaou, and N. Yamamoto, *Angew. Makromol. Chem.*, **221**, 67 (1994).
19. I. Arvanitoyannis, E. Nikolaou, and N. Yamamoto, *Polymer*, **35**, 4678 (1994).
20. I. Arvanitoyannis, E. Nikolaou, and N. Yamamoto, *Macromol. Chem. Phys.*, to appear.
21. D. M. Bigg and J. R. Preston, *Polym. Compos.*, **10**, 261 (1989).
22. K. Friedrich and U. A. Karsch, *Polym. Compos.*, **3**, 65 (1982).
23. E. Jinen, *J. Mater. Sci.*, **22**, 1956 (1987).
24. M. G. Bader, in *Handbook of Composites*, Vol. 4, A. Kelly, E. Yu, and N. Rabotnov, Eds., North Holland, Amsterdam, New York, Oxford, 1983, pp. 177-213.
25. V. K. Srivastava and S. Lal, *J. Mater. Sci.*, **26**, 6693 (1991).
26. I. Arvanitoyannis and E. Psomiadou, *J. Appl. Polym. Sci.*, **51**, 1883 (1994).
27. I. Arvanitoyannis, E. Nikolaou, E. Psomiadou, J. M. V. Blanshard, and N. Yamamoto, *Polymer*, to appear.
28. A. Vaxman, M. Narkis, A. Siegman, and S. Kenig, *Polym. Compos.*, **10**, 449 (1989).
29. G. Ives, J. Mead, and M. Riley, *Handbook of Plastics Test Methods*, Iliffe, London, 1971, p. 75, ASTM D792-66.
30. A. H. Kehayoglou and I. Arvanitoyannis, *Eur. Polym. J.*, **26**, 261 (1990).
31. D. E. Spahr and J. M. Schultz, *Polym. Compos.*, **11**, 201 (1990).

32. I. Arvanitoyannis, E. Psomiadou, J. M. V. Blanshard, and N. Yamamoto, *Polymer*, to appear.
33. C. K. Vonk, *J. Appl. Crystallogr.*, **6**, 148 (1973).
34. S. Kavesh and J. M. Schultz, *J. Polym. Sci. A-2*, **8**, 243 (1976).
35. J. M. Felix and P. Gatenholm, *J. Mater. Sci.*, **29**, 3043 (1994).
36. D. Campbell and Qayum, *J. Mater. Sci.*, **12**, 1427 (1977).
37. S. F. Xavier and Y. N. Sharma, *Angew. Makromol. Chem.*, **127**, 145 (1984).
38. A. J. Waddon, M. J. Hill, A. Keller, and D. J. Blundell, *J. Mater. Sci.*, **22**, 1773 (1987).
39. N. A. Mehl and L. Rebenfeld, *J. Polym. Sci. B, Polym. Phys.*, **31**, 1687 (1993).
40. W. Lee, B. Fukai, J. Seferis, and I. Chang, *Composites*, **19**, 473 (1988).
41. G. Titomanlio, S. Piccaloro, and G. Marrucci, *Polym. Eng. Sci.*, **25**, 91 (1985).
42. R. J. Watson and C. E. Chaffey, *Polym. Compos.*, **7**, 442 (1986).
43. C. D. Han, *Multiface Flow in Polymer Processing*, Academic Press, New York, 1981, Chap. 6.
44. S. Y. Hobbs, *Polym. Eng. Sci.*, **16**, 270 (1976).
45. W. B. Hillig, *J. Mater. Sci.*, **29**, 419 (1994).
46. W. B. Hillig, *J. Mater. Sci.*, **29**, 899 (1994).
47. J. Jancar, A. T. Dibenedetto, and A. J. Goldberg, *J. Mater. Sci.: Mater. Med.*, **4**, 562 (1993).
48. Y. Termonia, *J. Polym. Sci. B, Polym. Phys.* **32**, 969 (1994).
49. N. Sato, T. Kurauchi, S. Sato, and O. Kamigaito, *J. Mater. Sci.*, **26**, 3891 (1991).
50. Z. A. M. Ishak and J. P. Berry, *J. Appl. Polym. Sci.*, **51**, 2145 (1994).
51. M. J. Folkes, *Short Fiber Reinforced Thermoplastics*, Research Studies Press, Wiley, Chichester, 1982.
52. D. W. Van Krevelen, *Properties of Polymers*, 3rd ed., Elsevier, Amsterdam, 1990, pp. 367-454.
53. J. R. Lager and R. R. June, *J. Compos. Mater.*, **3**, 48 (1969).
54. O. Ishai, *Polym. Eng.*, **15**, 486 (1975).
55. A. Apicella, L. Nicolais, G. Astarita, and E. Drioli, *Polymer*, **20**, 1143 (1979).
56. M. L. Shiao, S. V. Nair, P. D. Garrett, and R. E. Pollard, *J. Mater. Sci.*, **29**, 1739 (1994).
57. M. L. Shiao, S. V. Nair, P. D. Garrett, and R. E. Pollard, *J. Mater. Sci.*, **29**, 1973 (1994).
58. H. W. Starkweather, Jr., G. E. Moore, J. E. Hansen, T. M. Roder, and R. E. Brooks, *J. Polym. Sci.*, **21**, 189 (1956).

Received September 7, 1994

Accepted November 7, 1994